

Generation of two-color polarization-entangled optical beams with a self-phase-locked two-crystal optical parametric oscillator

Julien Laurat, Gaëlle Kellerz, Claude Fabre, Thomas Coudreau^z

Norman Bridge Laboratory of Physics 12-33, California Institute of Technology, Pasadena, CA 91125, USA

^zLaboratoire Kastler Brossel, Université Pierre et Marie Curie,

Case 74, 4 Place Jussieu, 75252 Paris cedex 05, France and

^xLaboratoire Matériaux et Phénomènes Quantiques, Université Denis Diderot,

Case 7021, 2 Place Jussieu, 75251 Paris cedex 05, France

(Dated: May 24, 2019)

A new device to generate polarization-entangled light in the continuous variable regime is introduced. It consists of an Optical Parametric Oscillator with two type-II phase-matched nonlinear crystals orthogonally oriented, associated with birefringent elements for adjustable linear coupling. We give in this paper a theoretical study of its classical and quantum properties. It is shown that two optical beams with adjustable frequencies and well-defined polarization can be emitted. The Stokes parameters of the two beams are entangled. The principal advantage of this setup is the possibility to directly generate polarization entangled light without the need of fixing four modes on beam splitters as required in current experimental setups. This device opens new directions for the study of light-matter interfaces and generation of multimode non-classical light and higher dimensional phase space.

PACS numbers: 03.67.Hk, 03.67.Mn, 42.65.Yj, 42.50.Dv

I. INTRODUCTION

Developing quantum memories constitutes an essential milestone on the route towards quantum communication networks. As it is difficult to directly store photons, the quantum information has to be stored in a material-based quantum system. A particularly promising application for polarization-entangled light is the ability to couple it with atomic ensembles: the algebra describing the quantum properties of polarized light via Stokes operators [1, 2, 3] is exactly the same as that describing the quantum properties of atomic spin both single or collective spins. Quantum state exchange between light fields and matter systems has been recently experimentally demonstrated [4, 5] and it has been shown that such systems can be used as quantum memories [6]. In addition, from a technical point of view, the use of polarization states offers simpler detection schemes, without the need for local oscillators. These features make the study and experimental generation of non-classical polarization states of first importance for continuous variable quantum communication.

Furthermore, the study of higher dimensional phase space is a fascinating and promising subject. Indeed, it has been shown that multimode non-classical light could be a very powerful tool for an efficient processing and transport of quantum information [7]. Already experimental implementations and applications of such non-classical multimode light have been demonstrated in the continuous-wave regime [8, 9, 10, 11]. Such systems ei-

ther involve a very large number of modes [10, 11] or a much smaller number (three in the case of ref. [9]). Increasing the number of correlated modes is of particular importance, for instance in the case of optical read-out technologies [12] and super-resolution techniques [13]. In this context, generating continuous-variable polarization-entangled light [1, 2, 3], which exhibits three or four mode correlations, is a first step towards increasing the phase space dimension.

Such polarization-entangled beams in the continuous variable regime have been recently produced experimentally with injected type-I phase-matched Optical Parametric Oscillators (OPOs) below threshold [14, 15] or using ⁽³⁾ effects in a cloud of cold atoms [16]. All these methods require linear interferences of two quadrature-entangled modes with two bright coherent states, which limits the amount of entanglement reached and the simplicity and scalability of the setup.

We investigate here a new approach to directly generate polarization-entangled light without the need of mode fixing. This approach stems from an original device we previously studied, a self-phase-locked optical parametric oscillator. This system consists of a type-II phase-matched nonlinear ⁽²⁾ crystal in an optical cavity and emits fields that are phase-locked through linear coupling [17, 18, 19]: a birefringent plate, which can be rotated relative to the principal axis of the crystal, adds this coupling between the orthogonally polarized signal and idler beams and results in a phase-locking phenomenon that is well-known for coupled mechanical or electrical oscillators [20]. Such systems have recently attracted a lot of attention as efficient sources of non-classical light [21, 22, 23]. Stable operation has been demonstrated experimentally even with very small coupling [17, 24, 25] and their non-classical properties are very encouraging

^zTo whom correspondence should be addressed (coudreau@spectro.jussieu.fr)

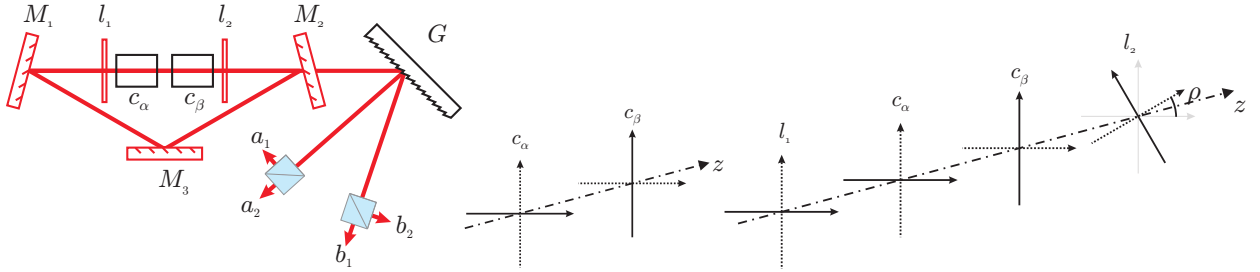


FIG. 1: Left: Ring cavity two o-crystal OPO : c_α , c_β are type-II nonlinear crystals, $l_{1,2}$ are $\lambda/2$ waveplates at ω_0 and ω_1 waveplates at ω_2 . $M_{1,3}$ are highly reflective mirrors at ω_0 and M_2 is a partially reflective mirror at ω_1 . All mirrors are transparent at ω_0 . G is a diffraction grating which separates the two frequency components. Each of them have two orthogonally-polarized bright components. Center: neutral axes seen by the fundamental wave at frequency ω_0 . Right: neutral axes seen by the sub-harmonic waves at frequencies ω_1 and ω_2 . Dotted lines denote fast axes and continuous lines slow axes.

[24]. We propose here a new implementation where two crystals, and not only one, are placed with their neutral axis orthogonal in a cavity containing two birefringent waveplates for adjustable linear coupling. Each crystal generates a pair of signal and idler beams and the waveplates couple together the two signal beams and the two idler beams so that phase locking can be achieved in a non-degenerate operation. As we will show below, this device allows for a direct and efficient generation of polarization-entangled optical beams.

In this paper, we investigate in detail the classical and quantum properties of the system. The paper is organized as follows. In Sec. II, we begin by presenting the linear and non-linear elements of the two-o-crystal OPO. A propagating Jones matrix is associated to each elements and permits to access the round-trip matrix and the stationary solutions. Section III considers the quantum properties of the emitted beams in terms of quadrature operators in the Fourier domain. The usual input-output linearization technique is used and quantum correlation spectra are formulated. In Section IV, these quadrature correlations are then interpreted in terms of polarization-entanglement through the Stokes operators. Considering various criteria, we demonstrate theoretically that this device is an efficient source of polarization-entanglement.

II. SET UP AND CLASSICAL PROPERTIES

In this section, we present the basic scheme of the two-o-crystal OPO. Round-trip equations and stationary solutions are then derived by using Jones matrix formalism.

A. Linear and non-linear elements in the OPO cavity

The setup is sketched in Fig. 1. Two identical type-II phase-matched ($^{(2)}$) crystals oriented at 90° and two birefringent waveplates are inserted inside a ring cavity. Signal and idler fields are resonant but the pump is not enhanced. The orientation of the various axes with respect to one another are critical. They are summarized on Fig. 1:

the nonlinear crystals c_α and c_β have their fast axes orthogonal;

waveplate l_1 has its fast axis parallel to the fast axis of the crystal c_α ;

the fast axis of the waveplate l_2 makes an angle with respect to the fast axis of crystal c_β . In this paper, we will restrict ourselves to small values of ρ .

Four fields may propagate inside the cavity: their classical amplitudes are denoted $a_{1,2}$ and $b_{1,2}$ where the index corresponds to the polarization and the letter to the frequency ω_a or ω_b (Fig. 1). The pump field is polarized at 45° of the crystals' axes and its amplitude is denoted a_0 . We consider that the pump and subharmonic fields are coupled via the nonlinear crystals. In c_α , the phase matching is such that $a_0^{(x)}$ is coupled to a_1 and b_2 while in c_β , $a_0^{(y)}$ is coupled to a_2 and b_1 .

We suppose that the waveplates for the subharmonic waves have identical dephasing for the two fields. M_1 and M_3 are highly reflective mirrors while the amplitude reflection coefficient for M_2 is denoted r . For the sake of simplicity, this coefficient is assumed to be real and independent of the frequency or of the polarization.

B. Propagation matrices

Birefringent elements are usually described by Jones matrices [26]. The total field can be decomposed into four components corresponding to the two subharmonic frequencies and the two linear polarizations. The waveplates l_1 and l_2 couple the fields a_1 and a_2 , and b_1 and b_2 independently while the crystals couple a_1 and b_2 , and a_2 and b_1 independently. Thus, the basis $|a_1; b_2; a_2; b_1\rangle$ is sufficient.

The waveplate l_1 is a $=2$ with its axes parallel to the basis axes so that its associated matrix is diagonal:

$$M_{l_1} = \begin{matrix} 0 & ie^{ik_a n_e} & 0 & 0 & 1 \\ B & 0 & ie^{ik_b n_e} & 0 & C \\ C & 0 & 0 & ie^{ik_a n_e} & A \\ 0 & 0 & 0 & ie^{ik_b n_e} & \end{matrix} \quad (1)$$

where $k_{a,b}$ denotes the wave vectors, n the mean index of refraction (dispersion is neglected) and e the thickness of the plate.

To determine the transfer matrix of the nonlinear crystals, the phase-matching will be taken perfect. We recall that the field amplitudes at the output of the first crystal can be written

$$a_1^{(out)} = a_1^{(in)} + g a_0^{(x)} b_2^{(in)}$$

$$\text{and } b_2^{(out)} = b_2^{(in)} + g a_0^{(x)} a_1^{(in)} \quad (2)$$

to the first order in g where $a_0^{(x)}$ denotes the pump amplitude at the output of the first crystal,

$$a_0^{(x)} = \frac{1}{2} a_0 \quad (3)$$

and where g is the nonlinear coupling coefficient given by

$$g = 1^{(2)} \frac{r}{2c^2 n_0 n_1 n_2} \frac{\sim!_0!_a!_b}{\sim!_0!_a!_b} : \quad (4)$$

Equations 2 are only valid close to the oscillation threshold where the pump depletion is small, which corresponds to the usual operation regime of such non-linear devices in quantum optics [24]. The transfer matrix of the first crystal takes thus the following form :

$$M_c = \begin{matrix} 0 & e^{ik_a n_1 l} & g \frac{a_0}{2} e^{ik_a n_1 l} & 0 & 0 & 1 \\ B & g \frac{a_0}{2} e^{ik_b n_1 l} & e^{ik_b n_1 l} & 0 & 0 & C \\ C & 0 & 0 & e^{ik_a n_2 l} & 0 & A \\ 0 & 0 & 0 & e^{ik_b n_2 l} & & \end{matrix} : \quad (5)$$

As stated before, perfect phase-matching has been assumed. $n_{1,2}$ stand for the refractive indices along the neutral axes and l is the crystal thickness. In the second crystal, only a_2 et b_1 are coupled to the pump. By assuming that the two crystals are at the same temperature, the transfer matrix is given by :

$$M_c = \begin{matrix} 0 & e^{ik_a n_2 l} & 0 & 0 & 0 & 1 \\ B & 0 & e^{ik_b n_2 l} & 0 & 0 & C \\ C & 0 & 0 & e^{ik_a n_1 l} & g a_0^{(y)} e^{ik_a n_1 l} & A \\ 0 & 0 & g a_0^{(y)} e^{ik_b n_2 l} & e^{ik_b n_2 l} & & \end{matrix} : \quad (6)$$

$a_0^{(y)}$ denotes the pump amplitude along y between the two crystals,

$$a_0^{(y)} = \frac{1}{2} a_0 : \quad (7)$$

Finally, the last waveplate is a $=2$ waveplate rotated by an angle $(\alpha + \beta = 2)$ with respect to l_1 . In the limit of small angles, the transfer matrix is found to be, to the first order in g [9]

$$M_{l_2} = \begin{matrix} 0 & ie^{ik_a n_e} & 0 & i_0 e^{ik_a n_e} & 0 & 1 \\ B & 0 & ie^{ik_b n_e} & 0 & i_0 e^{ik_b n_e} & C \\ C & i_0 e^{ik_a n_e} & 0 & ie^{ik_a n_e} & 0 & A \\ 0 & i_0 e^{ik_b n_e} & 0 & ie^{ik_b n_e} & & \end{matrix} : \quad (8)$$

where $\alpha + \beta = 2$.

As mentioned earlier, we assume that the mirror properties are independent both of the frequency and of the polarization. The free propagation matrix is thus

$$M_{\text{prop}} = \begin{matrix} 0 & e^{ik_a L} & 0 & 0 & 0 & 1 \\ B & 0 & e^{ik_b L} & 0 & 0 & C \\ C & 0 & 0 & e^{ik_a L} & 0 & A \\ 0 & 0 & 0 & e^{ik_b L} & & \end{matrix} : \quad (9)$$

where L is the cavity length without taking into account the birefringent elements (waveplates and crystal).

One can now calculate the round-trip matrix:

$$M_{\text{rt}} = M_{\text{prop}} M_{l_2} M_c M_{\text{c_alpha}} M_{l_1} : \quad (10)$$

Rather than giving the round-trip matrix in the general case, let us now make the following assumptions which are usually verified experimentally:

the loss for the subharmonic fields is high. The coefficient r is close to 1 and we put $r = 1$ with 1 ;

we assume that the double resonance condition is verified, that is both

$$a_{a,b} = k_{a,b} (L + 2ne + l(n_1 + n_2)) \quad (11)$$

are close to an integer multiple of 2π . We denote $\alpha_{a,b}$ their small round-trip phase detunings.

the waveplates l_1 and l_2 are $=2$ for the two frequencies ω_a and ω_b .

In this case, the round-trip matrix to the first order in $a_{a,b}; g$; and α takes the following form :

$$M_{\text{rt}} = \begin{matrix} 0 & 1 + i_a & g \frac{a_0}{2} & 0 & 0 & 1 \\ B & g \frac{a_0}{2} & 1 + i_b & 0 & 0 & C \\ C & 0 & 0 & 1 + i_a & g \frac{a_0}{2} e^{i\alpha_a} & A \\ 0 & 0 & 0 & g \frac{a_0}{2} e^{i\alpha_b} & 1 + i_b & \end{matrix} : \quad (12)$$

where $\alpha = (k_b n_1 + k_a n_2)l$. The phase of the pump amplitude between the two crystals has been shifted by $(k_a + k_b)ne$.

C. Stationary solutions

The stationarity of the solutions corresponds to the fact that the field amplitudes after one round trip must be

equal to the initial ones. This condition can be expressed in terms of the round-trip matrix:

$$M_{rt} \begin{pmatrix} 0 & a_1 & 1 & 0 & a_1 & 1 \\ B & b_2 & C & B & b_2 & C \\ a_2 & a_2 & A & a_2 & a_2 & A \\ b_1 & b_1 & B & b_1 & b_1 & B \end{pmatrix} = \begin{pmatrix} 0 & a_1 & 1 & 0 & a_1 & 1 \\ B & b_2 & C & B & b_2 & C \\ a_2 & a_2 & A & a_2 & a_2 & A \\ b_1 & b_1 & B & b_1 & b_1 & B \end{pmatrix} \quad (13)$$

For this system to have a non trivial solution, one must verify:

$$\det(M_{rt} - I) = 0: \quad (14)$$

The equation resulting from the stationarity condition 14 is similar to that obtained in a one-crystal self-phase locked OPO, which has been studied in detail in [18, 19, 25]. Let us briefly recall the main properties of this system: for a given incident pump intensity, the phase-locked operation can be obtained only for a given range of the relevant parameters (i.e. cavity length and crystal temperature) which defines a so-called locking zone. This locking zone is typically a cavity resonance width large in terms of length and a few tens of Kelvins in terms of temperature, well within experimental capacities. For a one-crystal self-phase locked OPO, phase-locked operation was indeed observed even for extremely small angles of the wave plate [24] where it does not perturb the quantum properties of the system [23].

Since we are interested in the quantum properties of the system, we will restrict ourselves to the lowest threshold region where $a = b = 0$, $\gamma = 0$ and

$$jga_0 \gamma^2 = 2^2: \quad (15)$$

In this case, the round-trip matrix is simpler and can be rewritten:

$$M_{rt} = \begin{pmatrix} 0 & & & & 1 & \\ 1+i_0 & & & & 0 & \\ B & & & & 0 & C \\ a & 1 & i_0 & 0 & 0 & C \\ 0 & 0 & 1+i_0 & 1+i_0 & 1 & A \\ 0 & 0 & & & 1 & i_0 \end{pmatrix} \quad (16)$$

The eigenvector of the round-trip equation, $M_{rt}J = J$, is given by

$$J = J \begin{pmatrix} 0 & 1 & 1 \\ B & 1 & C \\ a & i & A \\ i & & B \end{pmatrix} \quad (17)$$

where J is a (a priori complex) constant. This expression shows that the field generated consists in two modes at frequencies ω_a and ω_b with right circularly polarization. J is determined by the pump depletion equation:

$$a_0 = a_0^{in} g a_1 b_2 e^{ikn_0 l} \quad (18)$$

again to the first order in the nonlinear coupling coefficient g . If one fixes the pump phase between the two

crystals to be zero, this equation yields

$$\frac{r}{g_2} + g j \gamma \frac{\gamma^2}{f^2} = I_0^{(in)} \quad (19)$$

with $I_0^{(in)} = a_0^{(in)}$. One then gets the usual OPO solution:

$$J = \frac{r}{g^2} \left(-1 \right) e^{i \frac{\gamma}{f} l} \quad (20)$$

with

$$= \frac{g I_0^{(in)}}{t} = \frac{v}{t} \frac{u}{\frac{I_0^{(in)}}{I_0^{(threshold)}}}: \quad (21)$$

Eq. 15 shows that when the pump beam has a power larger than $2^2 = j \gamma^2 f^2$, four beams with fixed relative phases given by Eq. 17 are generated. Since the two signal (resp. idler) beams have a fixed phase relation and identical frequencies, they form a single beam with a circular polarization state. The system thus generates two circularly polarized beams which are frequency tunable and have a fixed phase relation between them.

The next sections are devoted to the study of the quantum properties. Correlations and anticorrelations of the couple signal/idler emitted by each crystal, i.e. $(a_1; b_2)$ or $(a_2; b_1)$, are formulated.

III. QUANTUM PROPERTIES AND QUADRATURE FLUCTUATIONS

In order to calculate the fluctuations for the involved fields when the system is pumped above threshold, we apply the usual input-output linearization technique (see e.g. [27]). Individual noise spectra as well as the correlations between any linear combinations of the various fluctuations are derived in the Fourier domain.

A. Linearized equations

We first determine the classical stationary solutions of the evolution equations: these solutions are denoted $a_i^{(s)}; b_j^{(s)}$ where $i = 0; 1; 2$; $j = 1; 2$. We then linearize the evolution equations around these stationary values by setting: $a_i = a_i^{(s)} + a_i$; $i = 0; 1; 2$ and $b_j = b_j^{(s)} + b_j$; $j = 0; 1$.

The evolution equations for the fluctuations are deduced from the round-trip matrix taking into account the stationary solutions 15, 17, 20:

$$\begin{aligned}
 \frac{d a_1}{dt} &= (- + i_0) a_1 + b_2 + e^{i-1} p \frac{1}{(-1)} a_0^{(x)} \stackrel{(in)}{=} +_0 a_2 e^{2i-1} (-1) b \frac{p}{2} \bar{a}_1^{in} \\
 \frac{d a_2}{dt} &= (- + i_0) a_2 + b_1 + ie^{i-1} p \frac{1}{(-1)} a_0^{(y)} \stackrel{(in)}{=} +_0 a_1 + e^{2i-1} (-1) b \frac{p}{2} \bar{a}_2^{in} \\
 \frac{d b_1}{dt} &= (- + i_0) b_1 + a_2 + ie^{i-1} p \frac{1}{(-1)} a_0^{(y)} \stackrel{(in)}{=} +_0 b_2 + e^{2i-1} (-1) a \frac{p}{2} \bar{b}_1^{in} \\
 \frac{d b_2}{dt} &= (- + i_0) b_2 + a_1 - e^{i-1} p \frac{1}{(-1)} a_0^{(x)} \stackrel{(in)}{=} +_0 b_1 - e^{2i-1} (-1) a \frac{p}{2} \bar{b}_2^{in}
 \end{aligned} \tag{22}$$

where τ stands for the cavity round-trip time. τ corresponds to the vacuum fluctuations entering the cavity through the coupling mirror.

The evolution equations can be then expressed in matrix form :

B. Quadrature fluctuations

We determine the amplitude and phase quadratures of a mode with mean phase α by respectively

$$\begin{aligned} p_a &= ae^{i/a} + a e^{i/a} \\ q_a &= i ae^{i/a} \quad ae^{i/a} : \quad (23) \quad \text{where} \end{aligned}$$

$$\frac{d}{dt} J = M - J + \frac{p}{2} \frac{1}{(J^{\text{in}} - J)} + \frac{p}{2} J^{\text{in}} \quad (24)$$

J is the column vector of the quadrature components

$$J = (p_{a_1}; q_{a_1}; p_{a_2}; q_{a_2}; p_{b_1}; q_{b_1}; p_{b_2}; q_{b_2}); \quad (26)$$

In the frequency domain, the equations become

J_0^{in} for the input pump fluctuations,

$$J_0^{in} = (p_0^{(x)^{in}}; q_0^{(x)^{in}}; p_0^{(y)^{in}}; q_0^{(y)^{in}}; p_0^{(y)^{in}}; q_0^{(y)^{in}}; p_0^{(x^{in})}; p_0^{(x^{in})}): \quad (27)$$

and J^{in} the for the vacuum fluctuations entering the cavity through the coupling mirror

$$J^{in} = (p_{a_1}^{in}; q_{a_1}^{in}; p_{a_2}^{in}; q_{a_2}^{in}; \\ p_{b_1}^{in}; q_{b_1}^{in}; p_{b_2}^{in}; q_{b_2}^{in}): \quad (28)$$

These differential equations are readily transformed into algebraic equations by taking the Fourier transform.

$$2i \quad J^r(\) = M^0 J^r(\) + \frac{r-1}{2} J_0^{in}(\) + \frac{r}{2} J^{in}(\): \quad (29)$$

where $\omega = \frac{1}{2} = \frac{1}{c}$ is the noise frequency normalized to the cavity bandwidth $c = \frac{2}{\omega}$ and $c = \frac{1}{\omega}$ is the normalized coupling constant. $\mathcal{T}(\omega)$, $\mathcal{T}_0^{\text{in}}(\omega)$ and $\mathcal{T}^{\text{in}}(\omega)$ are the Fourier transforms of the column vectors 26, 27,

28. The matrix M^0 is defined by

$$M^0 = \begin{array}{c|ccccc|ccccc} 0 & & & & & & 1 & & & & \\ \hline & c & 0 & c & & & & 0 & 0 & 2 & 0 \\ & c & & c & 0 & & & 0 & 0 & 0 & c \\ & 0 & c & & c & & & 2 & 0 & 0 & c \\ & c & 0 & c & & & & 0 & 0 & 0 & c \\ \hline & 0 & 0 & 2 & 0 & & & c & 0 & c & c \\ & 0 & 0 & 0 & & & & c & c & 0 & c \\ & & 2 & 0 & 0 & & & 0 & c & & c \\ & & 0 & 0 & 0 & & & c & 0 & c & c \\ \hline & 0 & 0 & 0 & & & & c & 0 & c & c \end{array} \quad (30)$$

C. Correlations and anticorrelations

In order to use the symmetry of the equations, one can introduce the symmetric and antisymmetric components

$$\begin{aligned} p &= \frac{1}{2} (p_{a_1}() + p_{b_2}()) \\ q &= \frac{1}{2} (q_{a_1}() + q_{b_2}()) \\ r &= \frac{1}{2} (p_{a_1}() - p_{b_2}()) \\ s &= \frac{1}{2} (q_{a_1}() - q_{b_2}()) \end{aligned} \quad (31)$$

and

$$\begin{aligned} p &= \frac{1}{2} (p_{a_2}() + p_{b_1}()) \\ q &= \frac{1}{2} (q_{a_2}() + q_{b_1}()) \\ r &= \frac{1}{2} (p_{a_2}() - p_{b_1}()) \\ s &= \frac{1}{2} (q_{a_2}() - q_{b_1}()) \end{aligned} \quad (32)$$

In a standard OPO, one expects intensity correlations and phase anti-correlations. Using our notations, this corresponds to having r and r as well as q and q squeezed [28]. This is also the case in a phase-locked OPO in the limit of small coupling [23].

As previously, the equations verified by these quantities can be expressed in matrix form. However, it is interesting to note that the sums are independent from the differences. Thus, one can write two sets of equations:

$$2i \quad w(\) = M \quad \begin{array}{c} r \\ \hline \end{array} \quad w(\) + \quad \begin{array}{c} r \\ \hline 2 \end{array} \quad w_{0,+}^{in}(\) + \quad \begin{array}{c} r \\ \hline 2 \end{array} \quad w_0^{in}(\) \quad (33)$$

where w are the column vector

$$\begin{aligned} w_+(\) &= (p(\); p(\); q(\); q(\)); \\ w_0(\) &= (r(\); r(\); s(\); s(\)); \end{aligned} \quad (34)$$

$$M_+ = \begin{array}{c|ccccc} 2 & 1 & 0 & c & c & c \\ \hline & 0 & 2 & 1 & c & c \\ & c & c & 2 & 0 & c \\ \hline & c & c & 0 & 2 & 1 \end{array};$$

$$M_0 = \begin{array}{c|ccccc} 0 & 2 & 0 & c & c & c \\ \hline & 0 & 2 & c & c & c \\ & c & c & 0 & 0 & c \\ \hline & c & c & 0 & 0 & 0 \end{array}; \quad (35)$$

w_0^{in} are the column vectors for the input pump fluctuations,

$$\begin{aligned} w_{0,+}^{in}(\) &= p_0^{(x)in}(\); p_0^{(y)in}(\); q_0^{(x)in}(\); p_0^{(y)in}(\) \\ w_0^{in}(\) &= (0; 0; 0; 0) \end{aligned} \quad (36)$$

and v^{in} the column vector for the input fluctuations entering the cavity through the coupling mirror

$$\begin{aligned} w_+^{in}(\) &= p^{in}(\); p^{in}(\); q^{in}(\); q^{in}(\) \\ w^{in}(\) &= r^{in}(\); r^{in}(\); s^{in}(\); s^{in}(\) \end{aligned} \quad (37)$$

These equations can be easily solved and one obtains the equations for the intracavity fluctuations. However, the relevant fluctuations are those outside the cavity. They can be easily calculated using the boundary condition on the output mirror:

$$f_{out} = tf - rf_{in} - \frac{p}{2} f - f_{in} \quad (38)$$

and the corresponding spectra are given by

$$S_f(\) = \begin{array}{c} D \\ \hline \end{array} f_{out}(\) \begin{array}{c} E \\ \hline \end{array} f_{out}(\) : \quad (39)$$

The expressions are identical for the two sets of spectra $S_{p,q,r,s}$ and $S_{p,q,r,s}$:

$$\begin{aligned}
S_{p_u}(\omega) &= 1 + \frac{1}{2(\epsilon^2 + (1-\epsilon)^2)} + \frac{\epsilon^2 + (1-\epsilon)^2}{2((\epsilon^2 + (1-\epsilon)^2)^2 + \epsilon^2)}; \\
S_{q_u}(\omega) &= 1 - \frac{1}{2(\epsilon^2 + (1-\epsilon)^2)} \frac{(1-\epsilon)^2 + \epsilon^2}{2(\epsilon^2 + (1-\epsilon)^2)^2}; \\
S_{r_u}(\omega) &= 1 - \frac{1}{2(1 + \epsilon^2)} \frac{\epsilon^2}{2(\epsilon^2 + (1-\epsilon)^2)^2}; \\
S_{s_u}(\omega) &= 1 + \frac{1}{2(\epsilon^2 + (1-\epsilon)^2)} \frac{\epsilon^2}{2(\epsilon^2 + (1-\epsilon)^2)^2}; \\
\end{aligned} \tag{40}$$

$u = ; .$

The behavior of the squeezed spectra, $S_{r_u}^{(out)}$ and $S_{q_u}^{(out)}$, is shown on Figure 2. For small coupling and low analysis frequency, one observes that the spectra go to zero which indicates the existence of very large correlations. As usual, the spectra go to one as ϵ goes to infinity: the correlations exist only within the cavity bandwidth or conversely, only when the integration time is larger than the field life time in the cavity. The increase of ϵ also results in a degradation of the correlations and anti-correlations: the wave-plate tends to mix the fields, and this phenomenon is increased as the coupling is increased. This phenomenon can be understood in terms of phase division: as the coupling is increased, the phase division is reduced which in turn reduces the intensity correlations. Finally, the phase anticorrelations (Fig. 2, left) are also degraded as the input pump power is increased: as ϵ is increased, the input pump noise becomes more and more important.

This analysis has been performed by studying the fields generated by each crystal. Since several frequencies are involved, such a measurement would require the use of multiple local oscillators or of dephasing cavities [29]. It is thus easier experimentally as well as more fruitful for quantum information purposes to study the beams at each frequency, namely the couples $(a_1; a_2)$ and $(b_1; b_2)$, which are circularly polarized.

IV. POLARIZATION ENTANGLEMENT GENERATION

The non-classical properties of the two-crystal OPO are now analyzed in terms of polarization fluctuations. Polarization entanglement generation is demonstrated using various criteria introduced in the literature.

A. Quantum Stokes parameters

Before describing the properties of the system, let us briefly recall the quantum picture for polarization properties. The polarization of light beams can be described

in the general case by the Stokes parameters [30]:

$$\begin{aligned}
S_0 &= I_x + I_y \\
S_1 &= I_x - I_y \\
S_2 &= I_{+45} - I_{-45} \\
S_3 &= I_{+} - I_{-} \\
\end{aligned} \tag{41}$$

where $I_{x,y,+45}, I_{-45}, I_{+45}, I_{+}$ describe the intensity along the $x, y, +45^\circ, -45^\circ, +$, and $-$ polarization. These four parameters are not independent but are instead linked by the relation

$$S_0^2 = S_1^2 + S_2^2 + S_3^2 \tag{42}$$

for a totally polarized field.

The quantum polarization properties are defined via the quantum counterparts of the Stokes parameters [1, 2]:

$$\begin{aligned}
\hat{S}_0 &= \hat{a}_x^{\dagger} \hat{a}_x + \hat{a}_y^{\dagger} \hat{a}_y \\
\hat{S}_1 &= \hat{a}_x^{\dagger} \hat{a}_x - \hat{a}_y^{\dagger} \hat{a}_y \\
\hat{S}_2 &= \hat{a}_x^{\dagger} \hat{a}_y + \hat{a}_y^{\dagger} \hat{a}_x = \hat{a}_{+45}^{\dagger} \hat{a}_{+45} + \hat{a}_{-45}^{\dagger} \hat{a}_{-45} \\
\hat{S}_3 &= i \hat{a}_y^{\dagger} \hat{a}_x - \hat{a}_x^{\dagger} \hat{a}_y = \hat{a}_{+}^{\dagger} \hat{a}_{+} + \hat{a}_{-}^{\dagger} \hat{a}_{-} \\
\end{aligned} \tag{43}$$

$(\hat{S}_1; \hat{S}_2; \hat{S}_3)$ verify commutation relations identical to those verified by orbital momentum operators:

$$[\hat{S}_i; \hat{S}_j] = 2i\hat{S}_k \tag{44}$$

where $i; j; k = 1; 2; 3$ are cyclically interchangeable. These relations result in three uncertainty relations,

$$\begin{aligned}
{}^2\hat{S}_1 - {}^2\hat{S}_2 &= h\hat{S}_3 i^2; \quad {}^2\hat{S}_2 - {}^2\hat{S}_3 = h\hat{S}_1 i^2; \\
{}^2\hat{S}_3 - {}^2\hat{S}_1 &= h\hat{S}_2 i^2; \\
\end{aligned} \tag{45}$$

where the notation ${}^2(\hat{X})$ correspond to the variance of the operator \hat{X} .

B. Entanglement criteria

In our case, Eq. 17 shows that the output beams are circularly polarized, thus $h\hat{S}_1^{a,b} i = 0 = h\hat{S}_2^{a,b} i$. It results

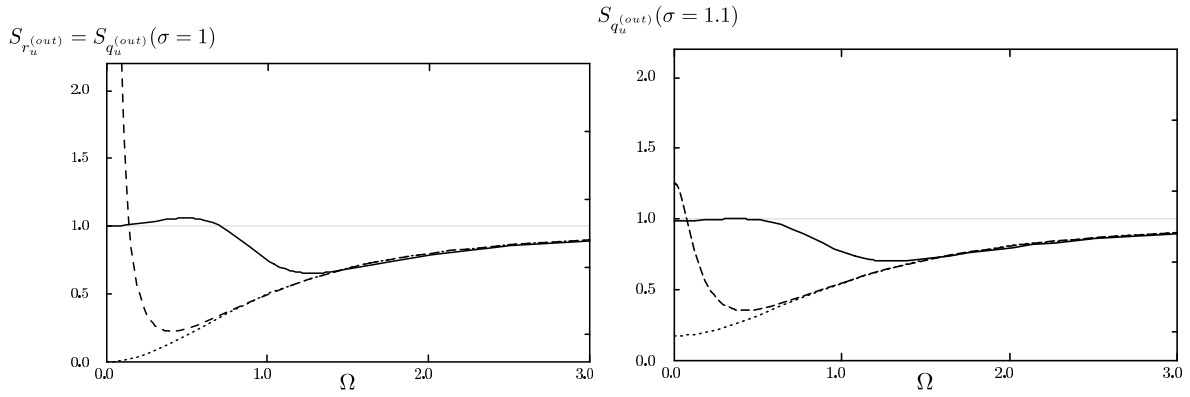


FIG. 2: Normalized noise spectrum of the amplitude quadrature difference and phase quadrature sum for $\sigma = 1$ (left) and $\sigma = 1.1$ (right). Continuous curves corresponds to $c = 1$, long-dashed to $c = 0.2$ and short-dashed to $c = 0$.

that the inequalities 45 which contain variances $\hat{S}_3^{a,b}$ are automatically verified. The only non-trivial Heisenberg inequality is then given by

$$2\hat{S}_1^{a,b} - 2\hat{S}_2^{a,b} - h\hat{S}_3^{a,b}i^2 = \frac{c}{g^2} (-1): \quad (46)$$

Various entanglement criteria have been defined. We will restrict ourselves to three of them [31, 32, 33, 34].

The first two criteria are, in the general case, sufficient (and not always necessary) conditions for entanglement. A general criterion is given by the product of two linear combinations of conjugate variables variances [33] (denoted "product criterion" in the following). In the case of the Stokes operators, this inseparability criterion states that when

$$2(\hat{S}_1^a - \hat{S}_1^b) : 2(\hat{S}_2^a - \hat{S}_2^b) - 2h\hat{S}_3^a i + h\hat{S}_3^b i \quad (47)$$

the state is entangled. The relevant Stokes parameters fluctuations, $\hat{S}_1^{a,b}$ and $\hat{S}_2^{a,b}$, can be expressed from the quadrature fluctuations. In the case of circularly polarized beams, one has ($u = a, b$)

$$\begin{aligned} \frac{\hat{S}_1^u(\omega)}{j\mathcal{J}} &= R_{u_1}^{(out)}(\omega) - R_{u_2}^{(out)}(\omega); \\ \frac{\hat{S}_2^u(\omega)}{j\mathcal{J}} &= (Q_{u_1}^{(out)}(\omega) - Q_{u_2}^{(out)}(\omega)): \end{aligned} \quad (48)$$

It follows from these expressions that:

$$\begin{aligned} \hat{S}_1^a(\omega) + \hat{S}_1^b(\omega) &= (R_{a_1}^{(out)}(\omega) - R_{b_2}^{(out)}(\omega)) - (R_{a_2}^{(out)}(\omega) - R_{b_1}^{(out)}(\omega)) = \frac{p}{2}(r^{(out)} - r^{(out)}) \\ \hat{S}_2^a(\omega) - \hat{S}_2^b(\omega) &= (Q_{a_1}^{(out)}(\omega) + Q_{b_2}^{(out)}(\omega)) + (Q_{a_2}^{(out)}(\omega) + Q_{b_1}^{(out)}(\omega)) = \frac{p}{2}(q^{(out)} + q^{(out)}) \end{aligned} \quad (49)$$

Thus the relevant spectra can be calculated from the previously calculated linear combinations of the amplitude

and phase quadrature components. They are given by:

$$\begin{aligned} S_{S_1^+}(\omega) &= 1 - \frac{c^2 - \mathcal{C}}{c^2 + (\mathcal{C}^2 - \mathcal{C})^2} \\ S_{S_2}(\omega) &= 1 - \frac{(\mathcal{C}^2 - \mathcal{C}) + (1 - 1)^2}{[c^2 + (1 - 1)^2 + \frac{c^2}{2} - 2\mathcal{C}^2 + (1 - 1)]^2 + \frac{4}{4}}: \end{aligned} \quad (50)$$

Let us remark that the two expressions are equal for $\mathcal{C} = 1$ and $c = 0$, i.e. for the uncoupled system operated at

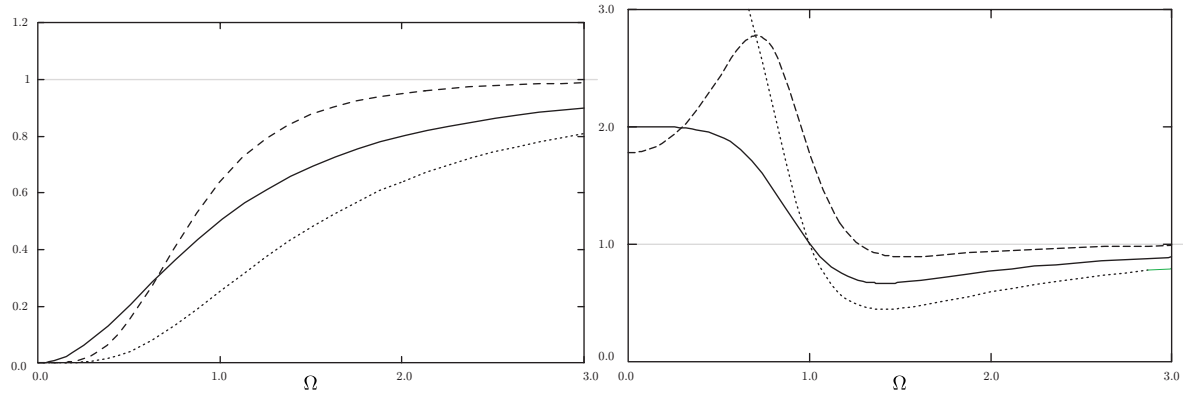


FIG. 3: Criterion spectra for $c = 0$ (left) and $c = 1$ (right). Continuous curves correspond to the sum criterion, long-dashed to the EPR criterion and short-dashed to the product criterion.

threshold.

The second criterion ("sum criterion"), which is widely used in continuous-variable entanglement characterization, is given by the sum of the above quantities [31, 32]. It is in fact a special case of the previous criterion [33]. The criterion states that if

$$\frac{1}{2} S_{S_1^+} + S_{S_2^-} \leq 1 \quad (51)$$

then the two states are entangled.

These two criteria are entanglement witnesses in the sense that they allow to specify whether the state is indeed entangled.

Finally, the last criterion is related to another particularity of the system which may allow to make a joint QND measurement of the two non-commuting observables \hat{S}_1 and \hat{S}_2 . It is shown in [34] that this is related to EPR-like "paradox". This criterion relies on conditional probabilities and can be written

$$S_{S_1^a} S_{S_2^b} \leq 1; \quad (52)$$

where

$$S_{S_i^a} S_{S_i^b} = h(S_i^a)^2 i - 1 - \frac{h(S_i^a)^2 h(S_i^b)^2}{h(S_i^a)^2 i h(S_i^b)^2} ; \quad i = 1, 2; \quad (53)$$

When this condition is verified, the correlations are sufficiently large that the information extracted from the measurement of the two Stokes operators of one field provides values for the Stokes operators of the other which violate the Heisenberg inequality [35].

Figure 3 shows the various criteria as a function of the analysis frequency, for a fixed pump power ($c = 1$) and for different values of the coupling. Very strong entanglement can be found for small couplings, c and small analysis frequencies, Ω . As the coupling is increased, the entanglement is shifted to higher values of the analysis frequency. Let us note however that $c = 1$ corresponds usually to large angles (around 1 for typical output couplers): in the case of single crystal phase locked OPOs, stable phase-locking has been achieved with very small

angles corresponding to $c = 0$. The entanglement is present for a wide range of the parameters thus showing the efficiency of the system.

V. CONCLUSION

We have presented and studied theoretically an original device based on an optical cavity containing two type-II phase-matched ⁽²⁾ crystals as well as birefringent plates which add a linear coupling between the signal and idler fields emitted in each crystal. The coupling induces a phase-locking respectively between the two signal fields and between the two idler fields. In this configuration, the system is found to directly generate two-color polarization-entangled beams without the need for mode mixing. The two-crystal OPO would be thus a useful resource for the field of continuous-variable quantum information. Non-classical polarization states are well coupled to atomic ensembles which can be used as quantum memories and form the basic block required for quantum networks. Furthermore, we believe that the experimental implementation of this device is very interesting for potential parallel processing as it would be a new step towards extending the dimension of the phase space experimentally accessible.

Acknowledgments

Laboratoire Kastler-Brossel, of the Ecole Normale Supérieure and the Université Pierre et Marie Curie, is associated with the Centre National de la Recherche Scientifique (UMR 8552). Laboratoire Matériaux et Phénomènes Quantiques, of Université Denis Diderot, is associated with the Centre National de la Recherche Scientifique (UMR 7162).

We thank A. Gatti for pointing us to ref. [33] and acknowledge fruitful discussions with G. Adesso and A. Serafini.

[1] A.S. Chirkov, A.A. Orlov, D.Yu. Parsons, Quantum theory of two-mode interactions in optically anisotropic media with cubic nonlinearities: Generation of quadrature- and polarization-squeezed light, *Kvant. Elektron.* 20, 999 (1993) *Quantum Electron.* 23, 870 (1993)

[2] N.Korolkova, G.Leuchs, R.Loudon, T.C.Ralph, C.Silberhorn, Polarization squeezing and continuous-variable polarization entanglement, *Phys. Rev. A* 65, 052306 (2002)

[3] N.Korolkova, R.Loudon, Nonseparability and squeezing of continuous polarization variables, *Phys. Rev. A* 71, 032343 (2005)

[4] B.Julsgaard, J.Sherson, J.I.Cirac, J.Fiurasek, and E.S. Polzik, Experimental demonstration of quantum memory for light, *Nature*, 432, 482 (2004).

[5] M.D.Lukin, Trapping and manipulating photon states in atomic ensembles, *Rev. Mod. Phys.* 75, 457 (2003).

[6] A.Dantan, A.Bramati and M.Pinard, Entanglement storage in atomic ensembles, *Europhys. Lett.* 67, 881 (2004).

[7] A.Gatti, I.V.Sokolov, M.I.Kolobov, L.A.Lugiato, Quantum fluctuations in holographic teleportation of optical images, *Eur. Phys. J. D* 30, 123 (2004)

[8] M.Martinelli, N.Treps, S.Ducci, S.Gigan, A.Mattre, C.Fabre, Experimental study of the spatial distribution of quantum correlations in a confocal optical parametric oscillator, *Phys. Rev. A* 67, 023808 (2003)

[9] N.Treps, N.Grosse, W.P.Bowen, C.Fabre, H.A.Bachor, P.K.Lam, A Quantum Laser Pointer, *Science*, 940 (2003)

[10] O.Jedrkiewicz, Y.-K.Jiang, E.Brambilla, A.Gatti, M.Bache, L.A.Lugiato, P.DiTrapani, Detection of Sub-Shot-Noise Spatial Correlation in High-Gain Parametric Down Conversion, *Phys. Rev. Lett.* 93, 243601 (2004)

[11] A.Mosset, F.Devaux, E.Lantz, Spatially Noiseless Optical Amplification of Images, *Phys. Rev. Lett.* 94, 223603 (2005)

[12] V.Daubert, N.Treps, C.Fabre, Optical storage of high density information beyond the diffraction limit: a quantum study, manuscript in preparation

[13] V.N.Beskrovnyy and M.I.Kolobov, Quantum limits of super-resolution in reconstruction of optical objects, *Phys. Rev. A* 71, 043802 (2005)

[14] W.P.Bowen, N.Treps, R.Schnabel, P.K.Lam, Experimental demonstration of continuous variable polarization entanglement, *Phys. Rev. Lett.* 89, 253601 (2002)

[15] R.Schnabel, W.P.Bowen, N.Treps, T.Ralph, H.A.Bachor, P.K.Lam, Stokes-operator-squeezed continuous-variable polarization states, *Phys. Rev. A* 67, 012316 (2003).

[16] V.Josse, A.Dantan, A.Bramati, E.Giacobino, Entanglement and squeezing in a two-mode system: theory and experiment, *J. Opt. B: Quant. Semiclass. Opt.* 6, S532 (2004)

[17] E.J.Mason, N.C.Wong, Observation of two distinct phase states in a self-phase-locked type II phase-matched optical parametric oscillator, *Opt. Lett.* 23, 1733 (1998)

[18] C.Fabre, E.J.Mason, N.C.Wong, Theoretical analysis of self-phase locking in a type II phase-matched optical parametric oscillator, *Opt. Comm.* 170, 299 (1999)

[19] L.Longchambon, J.Laurat, T.Coudreau, C.Fabre, Nonlinear and quantum optics of a type II OPO containing a birefringent element, 1. Classical operation, *Eur. Phys. J. D* 30, 279 (2004)

[20] A.Pikovsky, M.Rosenblum, J.Kurths, *Synchronization* (Cambridge U.Press, Cambridge, England, 2001).

[21] L.Longchambon, J.Laurat, N.Treps, S.Ducci, A.Mattre, T.Coudreau, C.Fabre, Production de faisceaux EPR a l'aide d'un OPO a auto-verrouillage de phase, *J. Phys. IV France* 12, P15-147 (2002)

[22] H.H.Adamyan, G.Yu.Kryuchyan, Continuous-variable entanglement of phase-locked light beams, *Phys. Rev. A* 69, 053814 (2004)

[23] L.Longchambon, J.Laurat, T.Coudreau, C.Fabre, Nonlinear and quantum optics of a type II OPO containing a birefringent element, 2. bright entangled beams generation, *Eur. Phys. J. D* 30, 287 (2004)

[24] J.Laurat, T.Coudreau, L.Longchambon, C.Fabre, Experimental observation of quantum correlations in a type II OPO above threshold: beyond the non-degenerate operation, *Opt. Lett.* 30, 1177 (2005)

[25] P.Gro, K.-J.Boller, M.E.Klein, High-precision wavelength-selective frequency division for metrology, *Phys. Rev. A* 71, 043824 (2005)

[26] R.C.Jones, A new calculus for the treatment of optical systems, *J. Opt. Soc. Am.* 31, 488 (1941)

[27] C.Fabre, E.Giacobino, A.Heidmann, L.Lugiato, S.Reynaud, M.Vadacchino, and W.Kaige, Squeezing in detuned degenerate optical parametric oscillators, *Quantum Opt.* 2, 159 (1990)

[28] S.Reynaud, C.Fabre, E.Giacobino, Quantum fluctuations in a two-mode parametric oscillator, *J. Opt. Soc. Am. B* 4, 1520 (1987)

[29] A.S.Villar, L.S.Cruz, K.N.Cassemiro, M.Martinelli, and P.Nussenzveig, Generation of Bright Two-Color Continuous Variable Entanglement, *quant-ph/0506139* (2005)

[30] G.G.Stokes, On the Composition and Resolution of Streams of Polarized Light From Different Sources, *Trans. Cambridge Philos. Soc.* 9, 399 (1852)

[31] L.-M.Duan, G.Giedke, J.I.Cirac, and P.Zoller, Inseparability Criterion for Continuous Variable Systems, *Phys. Rev. Lett.* 84, 2722 (2000)

[32] R.Simon, Peres-Horodecki separability criterion for continuous variable systems, *Phys. Rev. Lett.* 84, 2726 (2000)

[33] V.Giovannetti, S.Mancini, D.Vitali, and P.Tombesi, Characterizing the entanglement of bipartite quantum systems, *Phys. Rev. A* 67, 022320 (2003)

[34] M.D.Reid, P.Drummond, Quantum Correlations of Phase in Nondegenerate Parametric Oscillation, *Phys. Rev. Lett.* 60, 2731 (1988)

[35] N.Treps and C.Fabre, Criteria of quantum correlation in the measurement of continuous variables in optics, *Laser Physics* 15 (Special Issue Dedicated to Professor Herbert Walther on His 70th Birthday Anniversary), 187 (2005)